DRAG DE-ORBIT DEVICE (D3) MISSION FOR VALIDATION OF CONTROLLED SPACECRAFT RE-ENTRY USING AERODYNAMIC DRAG

Sanny Omar[*], David Guglielmo[†], and Riccardo Bevilacqua[‡]

The miniaturization of technology has led to an increasingly capable body of small satellites such as CubeSats which have fueled a demand for affordable yet reliable miniaturized attitude and orbit control systems. The more relaxed control requirements typically relevant to CubeSats missions open the door for innovative technologies that can replace large and expensive legacy attitude control and propulsion systems. The steadily increasing number of actors in space has also made orbital debris handling and mitigation increasingly important. This includes reducing the amount of debris, minimizing the risk of in-space collisions, and minimizing the hazards to persons and property on the ground from debris re-entry.

The University of Florida Advanced Autonomous Multiple Spacecraft (ADAMUS) lab has developed a Drag De-Orbit Device (D3) for CubeSats consisting of retractable tape-spring booms that provide a drag area of .5 m^2 and can de-orbit a 12U, 15 kg CubeSat from a 700 km circular orbit in 25 years. By modulating the D3 drag area, orbital maneuvering can be performed and the host satellite can be made to de-orbit in a desired location. In addition, the dart configuration of the booms ensures that the host satellite will aerodynamically stabilize in the ram direction with the help of initial rate damping by magnetorquers contained in the D3. By partially retracting two booms opposite each other, the D3 equipped spacecraft will have a clear minimum moment of inertia axis which gravity gradient torques will work to align with the nadir vector. These gravity gradient and aerodynamic torques together can provide passive 3-axis attitude stabilization.

This paper details the design of a 2U CubeSat and mission that will be launched to validate the D3 and the orbital maneuvering, targeted re-entry, collision avoidance, and attitude stabilization algorithms developed by the ADAMUS lab. The targeted re-entry and orbital manevuering algorithms have been tested extensively through Monte Carlo simulations and collision avoidance algorithms are currently in development. The CubeSat will consist of a standard 1U structure containing a power system, battery, GPS, UHF radio, and D3 control board with the D3 subsystem mounted to the back to achieve a 2U form factor. The search for CubeSat launch opportunities is still in progress, but the team hopes to have the satellite deployed from the International Space Station. Tests of orbital maneuvering and collision avoidance algorithms will commence after de-tumble, boom deployment, and communication with the ground. Approximately two weeks before the expected re-entry, the targeted de-orbit algorithm will steer the satellite to a desired re-entry location visible by a JSpOC radar station. The radar tracking data along with GPS telemetry will be utilized to characterize the performance of the system and algorithms, update re-entry aero-thermodynamic models, and gauge the effectiveness of atmospheric density estimation techniques.

[*]PhD Candidate, Mechanical and Aerospace Engineering, University of Florida, 939 Sweetwater Dr., Gainesville, FL 32611

[†]Post-Doc, Mechanical and Aerospace Engineering, University of Florida, 939 Sweetwater Dr., Gainesville, FL 32611

[‡]Associate Professor, Mechanical and Aerospace Engineering, University of Florida, 939 Sweetwater Dr., Gainesville, FL 32611

INTRODUCTION

The increasing number of space vehicles launched has led to an increasing concern with orbital debris mitigation.[1] NASA requirements[2] state that low Earth orbit (LEO) spacecraft must de-orbit within 25 years and that the probability of human casualty from re-entering debris must be less than 1 in 10,000. Aerodynamic drag presents itself as a convenient and efficient way to expedite de-orbit and control the re-entry location of a LEO spacecraft without using thrusters. While several teams have developed drag devices and tested them in orbit,[3–5] the majority of these devices have been single-use drag sails that cannot be retracted. These devices had been developed with the sole purpose of expediting the de-orbit of a host satellite. The PADDLES retractable drag sail was developed previously by the University of Florida ADAMUS lab to facilitate orbital maneuvering,[6] but has not yet flown. The ExoBrake drag device[7,8] developed by NASA Ames deploys in a parachute shape and can be partially retracted, but is limited by how far it can retract and how many deploy-retract cycles it can perform. The ExoBrake is thus far the only drag device launched that can be utilized to perform orbital maneuvering,[9] but successful maneuvering with the ExoBrake has not been demonstrated so far and the controlled re-entry algorithms developed by that team involve uplinking a pre-computed set of desired ballistic coefficients to the satellite and applying these open loop.[9] In addition, while the ExoBrake provides passive aerodynamic stability if it is deployed while in the correct orientation, the ExoBrake is incapable of constraining rotation about the roll axis.[8] While multiple algorithms for orbital maneuvering using aerodynamic drag exist[10–13] and the Planet Labs has a CubeSat constellation with separation controlled by differential drag,[14] to date there has not been a successful controlled de-orbit of a spacecraft using entirely aerodynamic drag.

The University of Florida ADAMUS lab, with funding from the NASA Launch Services Program (LSP), has developed a new retractable drag de-orbit device (D3) capable of modulating the drag area of a host CubeSat while maintaining passive 3-axis stabilization using aerodynamic and gravity gradient torques.[6] The D3 can be utilized for orbital maneuvering, reduction of orbit lifetime, collision avoidance, and targeted re-entry. The ultimate goal of the D3 is to provide an affordable yet reliable and easy to integrate device that will enable LEO CubeSats to meet or exceed NASA debris mitigation requirements and will facilitate advanced CubeSat missions through enhanced attitude and orbit control. As a part of the project, a targeted re-entry algorithm has been developed that determines how the D3 should modulate its deployment level to re-enter the spacecraft in a desired location.[15] This algorithm offers improvements in robustness and reliability over the state of the art and is efficient enough to run onboard a CubeSat with a high performance processor such as a BeagleBone Black or Xiphos Q7. Feedback Control techniques are employed to ensure that the spacecraft follows a desired trajectory to the de-orbit point.[15] Algorithms for active collision avoidance are currently in development.

This paper discusses the design of the D3 mission which will involve the launch of a 2U CubeSat[16] equipped with the D3 device to test orbital maneuvering, collision avoidance, and targeted re-entry algorithms and validate the performance of the D3 device in space. The paper first gives an overview of the D3 device. next, the targeted re-entry algorithms and their expected performances are discussed. The next section details the planned spacecraft components and presents power and link analyses as well as thermal and shock/vibration test plans. Finally, the last two sections discus the mission concept of operations and the mission success criteria.

DRAG DE-ORBIT DEVICE (D3) OVERVIEW

The drag de-orbit device (or D3) consists of four retractable tape-spring booms inclined at 20 degrees relative to the face of the satellite to which the D3 is attached as shown in Fig. 1. A zoomed in view of the D3 device and an expanded view of one of the D3 deployers are shown in Fig. 2 and Fig. 3. The complete design of the D3 and the simulations utilized to inform this design are detailed by Guglielmo et al.[6] In summary, the "dart" configuration of the D3 booms allows the host satellite to aerodynamically stabilize such that the satellite z-axis (Fig. 1) is aligned with the velocity vector. Because the booms are 3.7 m long and about 4 cm wide, significant aerodynamic torques are created, facilitating aerodynamic stability up to an altitude of 700 km. The length of the booms and the ability to actuate each boom independently also allows two booms opposite each other to be partially retracted to create a clear minimum moment of inertia axis along the two deployed booms. Gravity gradient torques will work to passively align this minimum moment of inertia axis with the nadir vector. The combined effects of gravity gradient and aerodynamic torques enable the D3 to provide passive 3-axis attitude stabilization. To increase the attitude stability, three orthogonal magnetorquers are integrated into the D3 and serve to damp any attitude oscillations when set to run the B-Dot de-tumble algorithm discussed by Guglielmo et al.[6]

When fully extended the D3 increases the cross-wind surface area of the host satellite by .5 m^2 enabling a 12U, 15 kg CubeSat to de-orbit from a 700 km circular orbit in 25 years under standard atmospheric conditions. Unlike most other drag devices that can only be deployed once to increase the drag area, the D3 can be repeatedly retracted, facilitating orbital maneuvering, collision avoidance, and re-entry point targeting using aerodynamic drag. A prototype of a D3 deployer has been fatigue tested and functioned nominally after 500 full deploy retract cycles (more than would be required on an average mission) and continued to operate properly after thermal vacuum testing conducted to simulate the space environment.

RE-ENTRY POINT TARGETING ALGORITHM

The purpose of the D3 CubeSat mission is to test the ability of re-enter the atmosphere in a desired location by varying the spacecraft's aerodynamic drag through a modulation of the D3 booms. The drag modulation scheme necessary to de-orbit in the desired location is developed by Omar and Bevilacqua[15] and offers significant improvements over the state of the art.[9,17] The first step in the drag based re-entry scheme is the guidance generation algorithm. This technique calculates the drag profile that a spacecraft must maintain to de-orbit in a desired location. The calculation is done using the highest fidelity orbit propagator available and ensures that if the orbit propagator were a completely accurate reflection of reality, the spacecraft would de-orbit in the desired location if the prescribed boom deployment profile was applied. Unfortunately, even the best models are not perfect and there is significant uncertainty in the drag force prediction. For this reason, a guidance tracking algorithm[15] is utilized that varies the spacecraft's ballistic coefficient using an LQR-based full state feedback control methodology based on the linearized motion of the spacecraft relative to the guidance. An Extended Kalman Filter is utilized to remove sensor noise from the GPS-derived relative position and velocity estimates. This algorithm was tested using a Monte Carlo simulation approach with randomized initial condition and realistic models of drag uncertainty[18] and GPS sensor noise.[19] One thousand Monte Carlo simulations were conducted and in all cases, a guidance was generated that was trackable in a realistic environment. The average guidance error was 24.3 km with a standard deviation of 49.0 km and the average tracking error was 3.4 km down to a geodetic altitude of 90 km. All guidance errors were below 750 km and all tracking errors

were below 10 km. Fig. 4 and Fig. 5 show the results of the Monte Carlo guidance and tracking simulations and Fig. 6 shows the ballistic coefficient profile associated with one of the simulation runs. The D3 actuator was required to run for an average of 2.3% of the orbit lifetime based on the Monte Carlo simulations. 89 % of tracking simulations had an actuator run time below 3% of the total orbit lifetime when simulated with noise and perturbations greater than what can be expected for a real mission. The expected actuator run time and the required position and velocity knowledge determined from the simulations were utilized to determine the navigation system accuracy and power generation capability the CubeSat would require.

2U CUBESAT DESIGN

The D3 satellite is designed to test the D3 device and de-orbit point targeting algorithm. Secondary objectives will include the tests of other orbital maneuvering algorithms and collision avoidance algorithms. As such, to maximize the change of mission success, the 2U CubeSat will be built using TRL 9 parts (those with space legacy) whenever possible.

CubeSat Structure, Deployables, and Solar Panels

To maximize the chance of mission success, the CubeSat will be built around a standard 1U structure with significant space legacy designed an manufactured by Innovative Solutions in Space (ISIS). This 1U structure (Fig. 7) is designed with upper mounting holes which the manufacturer sometimes uses to convert it to a 1.5U structure. A custom-made adapter stage shown in Fig. 8 will be attached to these mounting holes and the D3 device will attach to the top of the adapter stage. All satellite avionics will be contained in the 1U structure. The adapter stage is manufacturable using the machines at the University of Florida ADAMUS lab and in addition to connecting the D3 to the standard 1U structure, ensures that the entire CubeSat is 225 mm long as required by the design standard.[16] The adapter vertical posts are manufactured separately from the bottom plate that attaches to the 1U structure. Prior to attachment to the 1U structure, four screws are utilized to connect the adapter base, through the adapter posts, to the D3 baseplate. The placement of the adapter over the 1U structure prevents these screws from falling out of place. The complete satellite assembly when the 1U structure, adapter stage, and D3 are connected is shown in Fig. 10.

A standard 1U solar panel manufactured by DHV technologies is located on top of the D3 deployer assembly which is designed to support this panel. The 2U faces of the satellite will contain solar panels custom made by DHV technologies to support the antenna deployment burn-wire, remove before flight pin, and USB charging and data cables. These panels will be fastened via screws to the standard solar panel mounting holes built into the 1U structure. The solar panels and their locations on the D3 CubeSat are shown in Fig. 9.

The 1U face of the satellite opposite the D3 system does not contain a solar panel, but instead hosts the pi-patch GPS antenna and the deployable Gomspace ANT430 UHF communication radio. The ANT430 deploys four quater-wave UHF (435 Mhz) antennas in a turnstile configuration that provides a nearly omni-directional signal pattern. Each antennas is secured to the solar panel PCB via a nylon wire that is wrapped around the antenna and around a nichrome burn wire that is attached using M2 screws to the solar panel PCB. Each antenna rests on an aluminum support component attached to the solar panel PCB such that the nylon wire is always in tension. When current is run through the nichrome wires that are connected in parallel to the 12V power bus through a controllable relay, the antennas simultaneously deploy.

CubeSat Avionics

Commercially available TRL 9 avionics are used in this satellite with the exception of the D3 control board that is custom-made. All avionics are integrated into the 1U structure which is manufactured with support for standard PC104 sized CubeSat boards.

COTS Avionics The D3 avionics are shown in Fig. 10 and the COTS (commercial off the shelf) avionics include the CPUT UTRX UHF half duplex radio board sold by Clyde Space, the piNAV-L1 GPS receiver made by SkyFox labs,[19] and 10 Whr Battery and Electrical Power System board from Clyde Space. The masses, costs, and expected power consumptions of these boards are shown in Table 1. With a maximum power output of 24 W, the EPS will be capable of running the D3 device, all avionics, and the radio simultaneously. The piNAV-L1 is the lowest power commercially available CubeSat GPS, and based on the Monte Carlo simulations discussed previously, will provide sufficient accuracy for the targeting algorithms. Note that all simulations were conducted with simulated measurement noise corresponding to the manufacturer specified values for the piNav-L1. The CPUT UTRX radio provides half duplex communication at 9600 bit/s on the 435 Mhz UHF band. The half duplex mode requires a single antenna on the ground and on the satellite for both reception and transmission. By connecting the UTRX to the ANT430 turnstile antenna, an omni-directional radiation pattern will be achieved whereby the satellite will be able to maintain contact with the ground regardless of its attitude.

D3 Control Board The D3 system will be controlled by a single board which will host a high performance processor that will also serve as the primary flight computer for the satellite. Currently, the team plans to use the Xiphos Q7 processor which is radiation tolerant, has spaceflight legacy, and contains a dual core, 766 Mhz Xilinx Zync processor. The Q7 will be more than capable of performing autonomous, onboard guidance generation and tracking and will connect to a PC104 sized PCB via a 90 pin mezzanine connector. This PCB will also contain four TI DRV8834 Low-Voltage Stepper Motor Driver chips to control the D3 stepper motors and two TI DRV8835 Dual Low-Voltage H-Bridge chips to control the magnetorquers. A 20 conductor ribbon cable will be connected to the D3 board to rout signals from the D3 board to the stepper motors and magnetorquers. Four cables will be required for each stepper and two for each magnetorquers. A TDK ICM-20948 9-axis IMU will also be included on the board. This chip uses only 2.4 mW and provides acceleration, angular velocity, and magnetic field measurements. These can be utilized with the magnetometers located on the solar panels for the B-Dot de-tumble algorithm. The D3 board will interface with the battery, EPS, GPS, and radio using the PC104 headers. Figure 11 shows the header pin configuration for the D3 board based on the interfacing requirements specified by the manufacturers of the other avionics.

Antenna Deployment Mechanism

The antenna deployment mechanism will be integrated into the solar panels as shown in Fig. 12 for simplicity and reliability. DHV technologies will manufacture each side (2U) solar panel with four unthreaded M2 holes for the antenna deployment mechanism. On each panel, two of the holes will be utilized to attach the bracket that the antenna rests on, and the other two will serve as screw terminals to attach the nichrome burn wire. The nichrome wire will loop around the screws on the outside of the solar panel and the nuts on the screws holding the nichrome wire will be utilized to attach strands of conductive wire that will be routed to standard screw terminals located on the D3 board. For each of the four deployable antennas, a loop of nylon wire tied in a surgeon's knot will attach to the nichrome wire such that the antenna is held in the stowed configuration. All four

nichrome burn wires will be connected in parallel such that the activation of a single relay on the D3 board will heat up all the nichrome wires which will cut the nylon lines and result in antenna deployment.

Mass, Power, and Financial Budgets

Table 1 shows the mass, power, and cost of each of the aforementioned spacecraft components. These values are given by the manufacturer for COTS components and are estimated based on the current stage of the design process for custom-made parts.

Detailed Power Analysis

AGI's System's Toolkit (STK) was utilized to determine the angle of the sun with respect to each face of the satellite at each point in time. For each solar panel, the produced power was calculated in terms of the maximum achievable power and the angle θ between the solar panel surface normal vector and the sun vector.

$$P = P_{max} \cos(\theta) \tag{1}$$

A power analysis is included for a space-station orbit (400 km circular at 51.9 degrees inclination) where the orbit angular momentum vector is perpendicular to the sun vector as shown in Fig 13. This orbit represents a worst case right ascension for power generation because it results in the maximum exposure of the 1U CubeSat faces to the sun and the minimum exposure of the 2U faces. This results in the lowest power generation because only one of the 1U faces has a solar panel and that panel generates only half the power of the 2U panels. Note that for the 2U side panels, $P_{max} = 4.24W$ and for the 1U top panel, $P_{max} = 2.12W$. The average power generation and total energy generated by each solar panel over the course of an orbit (5554 s) is shown in Table 2 and the power generation over time profile of each panel is shown in Fig. 14. Each solar panel is defined based on the spacecraft body axis (Fig. 1) that the normal vector of the panel aligns with. For example, the -x panel normal vector is aligned opposite the spacecraft body frame x-axis. Recall that this analysis represents a worst-case scenario for power generation. When the same power analysis was conducted for a scenario where the orbit angular momentum vector was as close as possible to parallel with the sun vector (right ascension shifted by 90 degrees), the average power generation was 3.83 W. Ideally, the deployment level of the drag device will be planned such that when it is time to begin the orbital maneuvering algorithm (about 2 weeks before de-orbit), the satellite will be in a maximum power orbit. Even if this is not possible, however, Table 1 shows that the expected orbit-averaged power consumption will remain under 2 W. Fig. 14 shows that the satellite will never be without power generation for more than an hour at any given time, so the 10 WHr battery should be sufficient for this mission and will not drain as long as the average power consumption is less than the average power generation. As a precaution however, logic will be built into the EPS and master micro-controller to reduce the electrical load in the event that battery charge drops below 50%.

Link Analysis

AGI's Systems Toolkit (STK) was utilized to assess the ability communicate with the satellite from the ground station. For the purpose of a worst case analysis, an isotropic ground antenna and the worst case gain of the ANT430 (-1dB) were considered. Atmospheric refraction and light travel time effects were also taken into account in the STK calculation. In this scenario, even when the spacecraft was located at an elevation of 5 degrees from the ground station in a 600 km circular

Table 1. Table of CubeSat Components with Masses and Power Usages

Component	Mass (g)	Avg Power User (mW)	Cost (USD)
Clyde Space 3rd Generation EPS	86	160	4,400
Clyde Space 10 WHr Battery	156	0	1,800
Clyde Space CPUT UTRX Half Duplex Radio	90	250 rx, 4000 tx, 333 avg with 30 min daily tx	8,600
GomSpace NanoCom ANT430 Communication Antenna	30	0	6,325
D3 Deployers	1100	200 avg, 15,000 peak	2,000
D3 Magnetorquers	101	Variable, max 1,000 during de-tumble	100
Xiphos Q7 Master CubeSat and D3 Micro-controller	24	1,000	18,000
DHV Technologies Custom Solar Panels (four 2U side panels, one 1U top panel)	400 g total	-4,240 max gen for 2U panels and -2,120 max gen for 1U panels	21,150
1U Innovative Solutions in Space Structure	200	0	2,560
D3 Adapter Stage	200	0	200
SkyFox piNav-L1 GPS Unit	100	139	9,300
SkyFox piPATCH GPS Antenna	25	100	2,237
Totals	2512	1,932 average continuous use	76,672

Table 2. Worst Case Power and Energy Generation Per Orbit for Each Solar Panel

Panel	+x	+y	+z	-x	-y	-z	Total
Orbit-Averaged Power Generation (W)	.0856	1.35	0	.134	0	.456	2.02
Energy Generated per Orbit (J)	476	7484	0	745	0	2532	11237

orbit (absolute worst case communication scenario), the signal to noise ratio was 10.8dB with 1 Watt of RF output power (3 Watt power draw) and the bit error rate was 1×10^{-6} using a 9600 bits/s downlink with GMSK modulation. With 2 W RF output power (5 W power draw), the signal to noise ratio was 12 dB and the bit error rate was 2.2×10^{-12}. With such a high link margin even in the worst case scenario, the team can be reasonably sure that it will be possible to reliably communicate with the satellite at any point where the satellite is physically in view of the ground station.

THERMAL ANALYSIS

The largest thermal concern in this mission is associated with the D3 device, specifically with the deployed booms. If untreated, the booms will have a solar absorptivity of 0.39 and emissivity of 0.11, resulting in maximum temperatures over 180 C. This would be unacceptably hot and may cause thermal warping of the booms or overheating of the boom deployment electronics. To remedy this, the booms will be treated to get an absorptivity to emissivity (A/E) ratio of 1 which will result in boom temperatures between -94 and 68 C which is acceptable.[6] Treatment options to achieve this A/E ratio include combined sandblasting and passivation, an aluminized film with silicon oxide coating, and the application of thermal paint. Exposed aluminum elements of the D3 device will be anodized to achieve an A/E ratio of 0.8, which yields acceptable temperatures. A plot of the expected temperatures over time (after treatment) of the D3 booms and aluminum D3 shells is shown in Fig 15.

The majority of the satellite will be covered in PCBs containing solar cells and the GPS patch antenna as shown in Fig. 9. Solar panels have an A/E ratio of approximately one[20] and thus, like the booms, will experience temperatures between -94 and 68 C in the most extreme cases. The panels are designed to operate between -120 C and 150 C, so this should not be an issue. In reality, the thermal fluctuations of the solar panels will be slightly smaller due to the minor thermal conductivity between the panels and the CubeSat structure which effectively adds some thermal inertia to the panels. The solar panels will also serve to shield the CubeSat avionics from large temperature swings that would otherwise occur due to thermal radiation. These panels and all CubeSat avionics except the D3 board are COTS components with spaceflight legacy, so no significant thermal issues are expected. Future work will include more detailed thermal modeling and analysis of the entire spacecraft with all components included.

Test Plans and Procedures

The spacecraft will require shock, vibration, and thermal vacuum (TVAC) testing as specified in the Launch Services Program Dispenser and CubeSat Requirements (LSP-REQ-317.01).[21] For qualification, the CubeSat and dispenser must be tested to four times the maximum predicted shock, sinusoidal vibration, and random vibration that will be experienced during the launch. These vibration values will depend on the launch platform which has not yet been determined, but it is likely that the CubeSat will launch through NanoRacks and be deployed from the Interntional Space Station. Preliminary structural analysis has indicated that the spacecraft can easily withstand the required shock and vibration test levels. In addition, the CubeSat must be simultaneously brought to a pressure less than 10^{-4} Torr and a temperature greater than 70 C. The CubeSat must be maintained at this temperature and pressure for at least three hours after thermal stabilization. The CubeSat will be in launch configuration (antenna stowed, all avionics integrated) for this testing. While this is the minimum required testing, specific launch providers may have additional testing requirements. Testing of key CubeSat functions, especially booms deployment, at the minimum and maximum

operating temperatures will also be conducted at pressures less than 10^{-4} Torr to ensure that the satellite will operate properly in the space environment.

After the TVAC, shock, and vibration testing, an operational test will be performed to ensure the CubeSat will still perform nominally after launch. To verify the functionality of the D3 board, EPS, and battery, hardware in the loop testing of all flight software and control algorithms will first be conducted. The antenna deployment mechanism will be tested after this to ensure reliable deployment after launch conditions. If that is successful, the CubeSat GPS and and radio will be tested to ensure to ensure that the GPS produces an accurate position and velocity measurement and the radio is capable of two-way communication with the ground station. Finally, the radio will be brought far away from the ground station (possibly in an airplane) and long-range communication capabilities will be tested.

MISSION CONCEPT OF OPERATIONS

The mission phases and conditions to go from one phase to the next are outlined in Fig. 16. The spacecraft will have on-orbit software update capabilities, so if any issues arise, ground operators can diagnose them and upload software patches. The current plan is to deploy the CubeSat from the International Space Station via NanoRacks, so the CubeSat is designed to conform to the NanoRacks payload specifications.[22] The team is planning to apply to the CubeSat Launch Initiative (CSLI) to secure funding for a launch and deployment through NanoRacks.

MISSION SUCCESS CRITERIA

The ultimate goal of the mission is to demonstrate targeted re-entry using aerodynamic drag. However, even if this objective is not successful, other useful technology demonstrations may still be completed including demonstrations of drag device deployment and operation in space, passive attitude stabilization, and orbital maneuvering using aerodynamic drag. Fig. 17 shows the contribution to overall mission success of the partial or total fulfillment of each of these objectives.

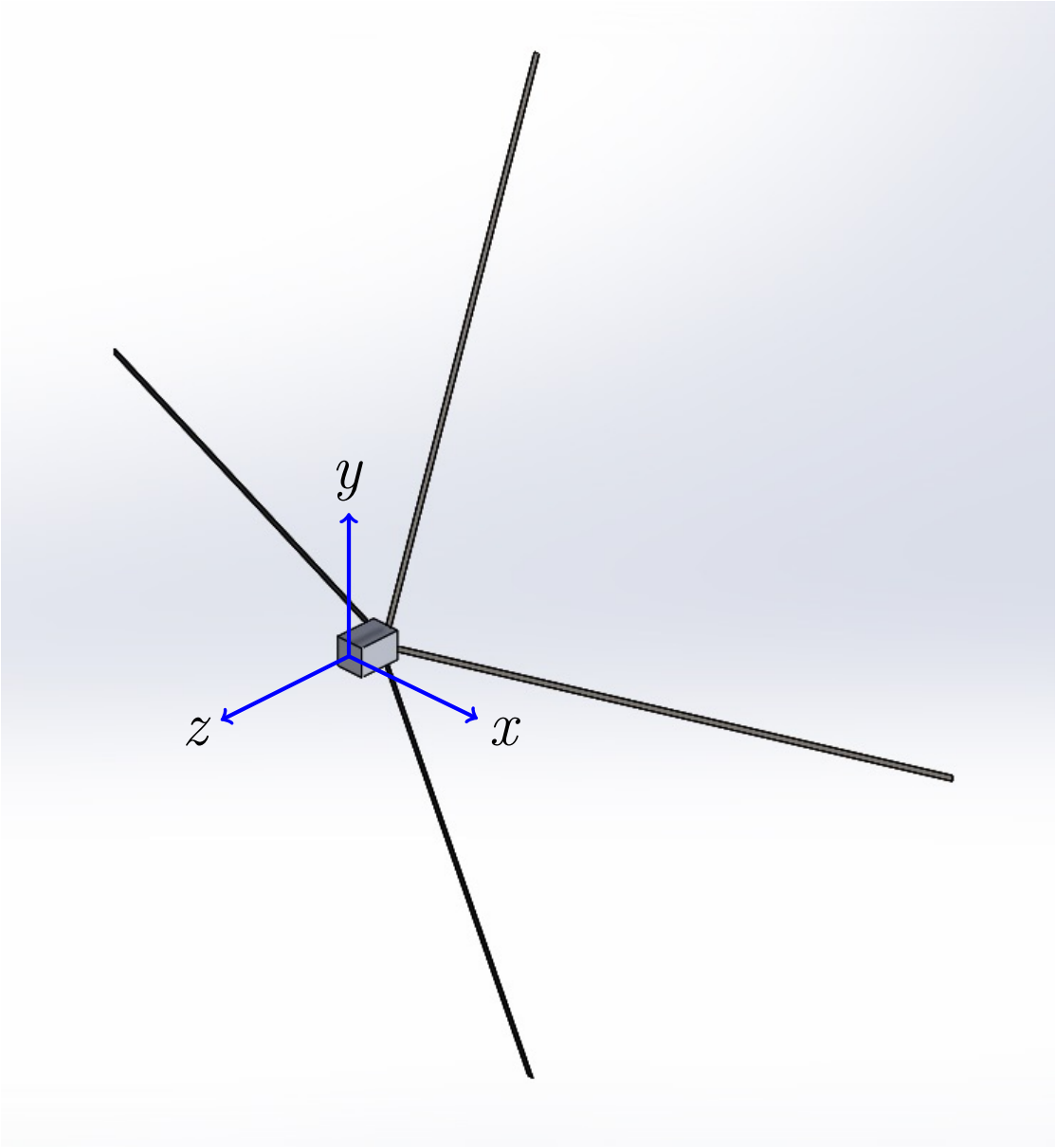

Figure 1. D3 Device Attached to a CubeSat with Body Axes Shown

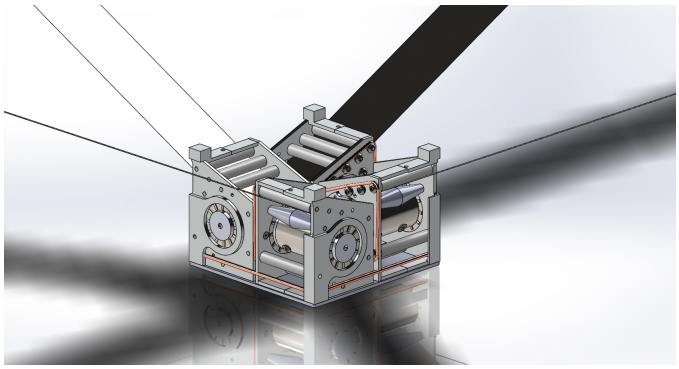

Figure 2. Zoomed in View of D3 Device

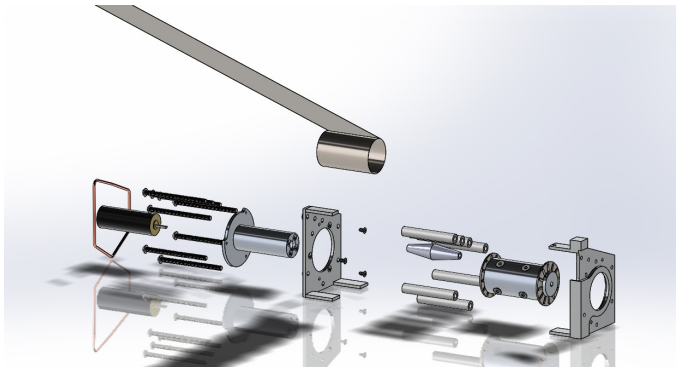

Figure 3. D3 Device Deployer Expanded View

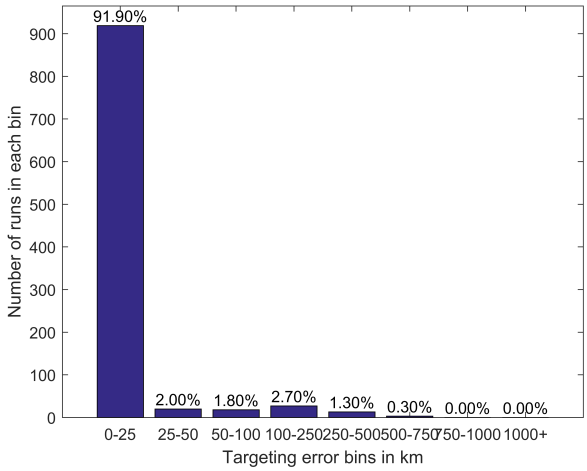

Figure 4. Monte Carlo Guidance Errors

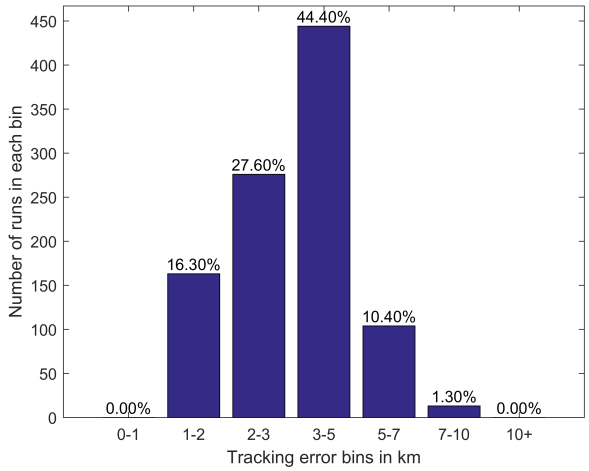

Figure 5. Monte Carlo Tracking Errors

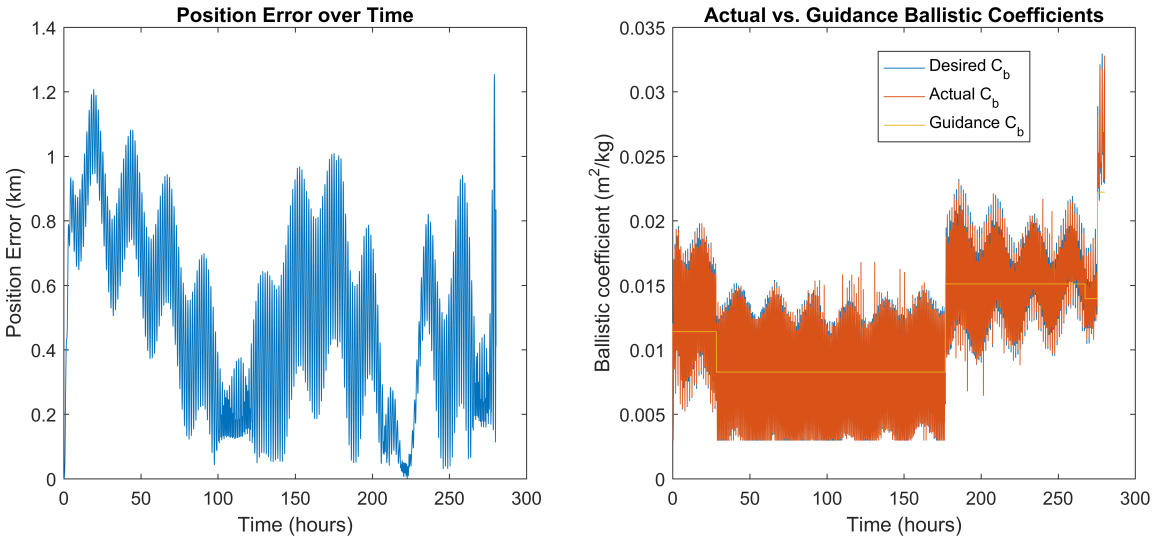

Figure 6. Position Error and Ballistic Coefficient over Time for Sample Simulation

Figure 7. Innovative Solutions in Space 1U Standard Structure

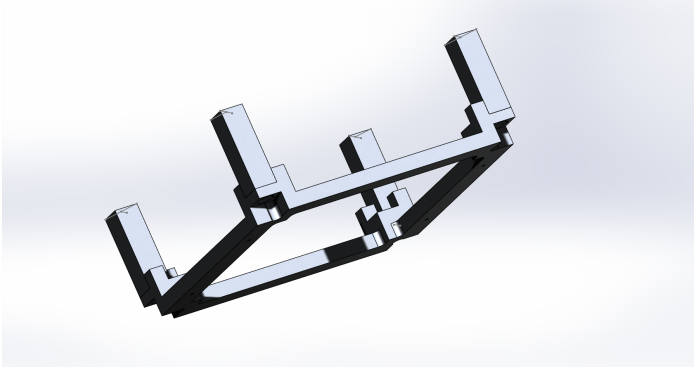

Figure 8. D3 Adapter

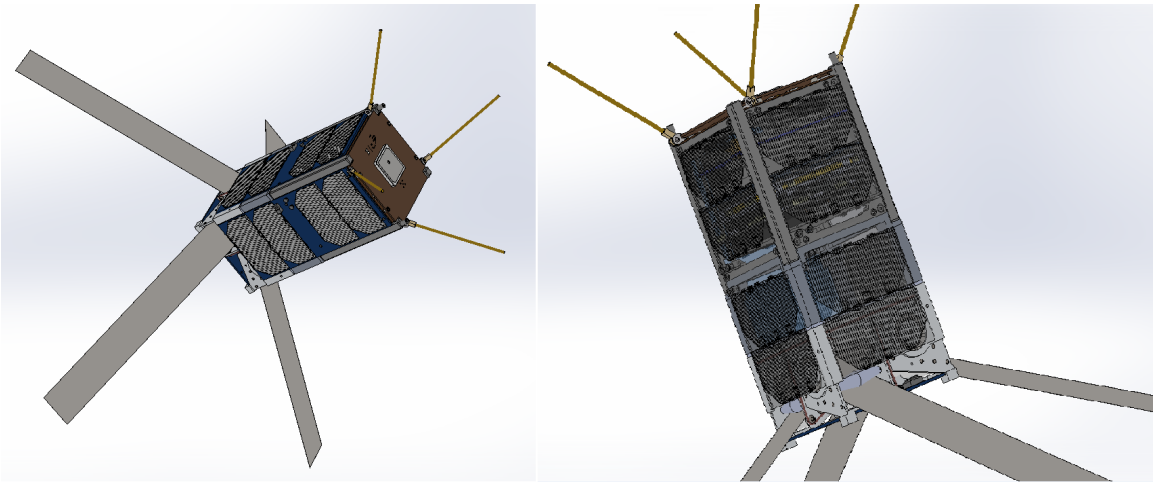

Figure 9. D3 CubeSat with Solar Panels

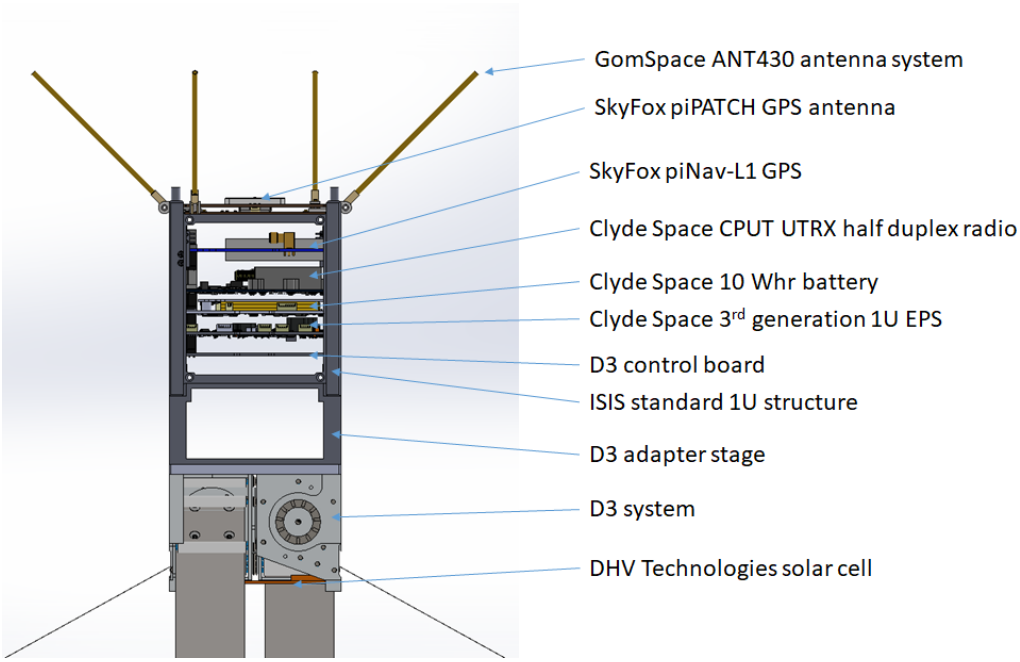

Figure 10. Complete CubeSat Structure with Integrated Avionics (No Side Solar Panels)

2	4	6	8	10	12	14	16	18	20	22	24	26	28	30	32	34	36	38	40	42	44	46	48	50	52
1	3	5	7	9	11	13	15	17	19	21	23	25	27	29	31	33	35	37	39	41	43	45	47	49	51

H2

2	4	6	8	10	12	14	16	18	20	22	24	26	28	30	32	34	36	38	40	42	44	46	48	50	52
1	3	5	7	9	11	13	15	17	19	21	23	25	27	29	31	33	35	37	39	41	43	45	47	49	51

H1

Key	
	USB Charge (H1-32)
	I2C Data (H1-41)
	I2C Clock (H1-43)
	Ground (H2-(9, 14, 17, 29, 30, 32, 47, 48))
	5V Regulated Power (H2-25, H2-26)
	3.3V Regulated Power (H2-27, H2-28)
	GPS Serial data receiver pin (H1-19)
	GPS Power on Signal (H1-23)
	GPS Power off Signal (H1-21)
	GPS Timing Pin (H1-45)
	GPS Position Fix Indicator (H1-49)
	Transmit Empty (H1-1)
	Transmit Ready (H1-5)
	Receive Ready (H1-6)
	Radio Reset (H1-2)
	Independent DTMF Pins (H2-(49-52))

Figure 11. D3 Board PC104 Pin Header Configuration

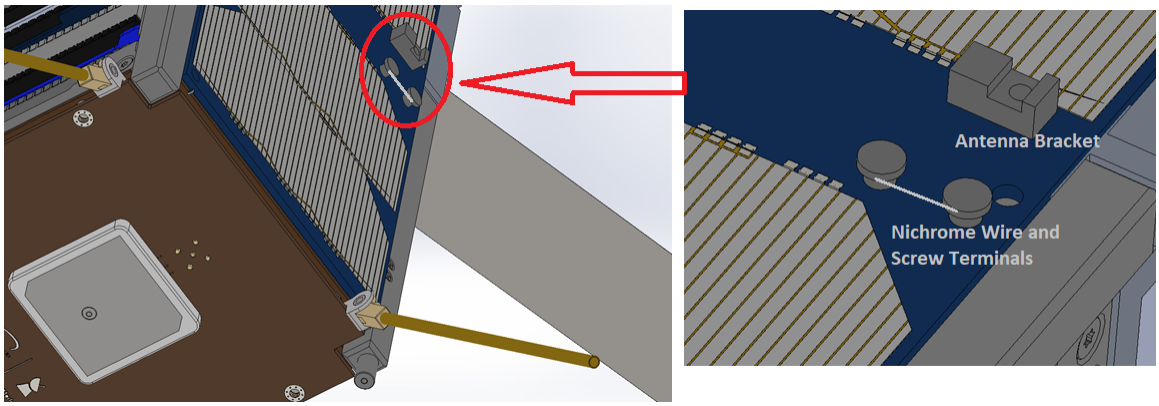

Figure 12. UHF Communications Antenna Deployment Mechanism

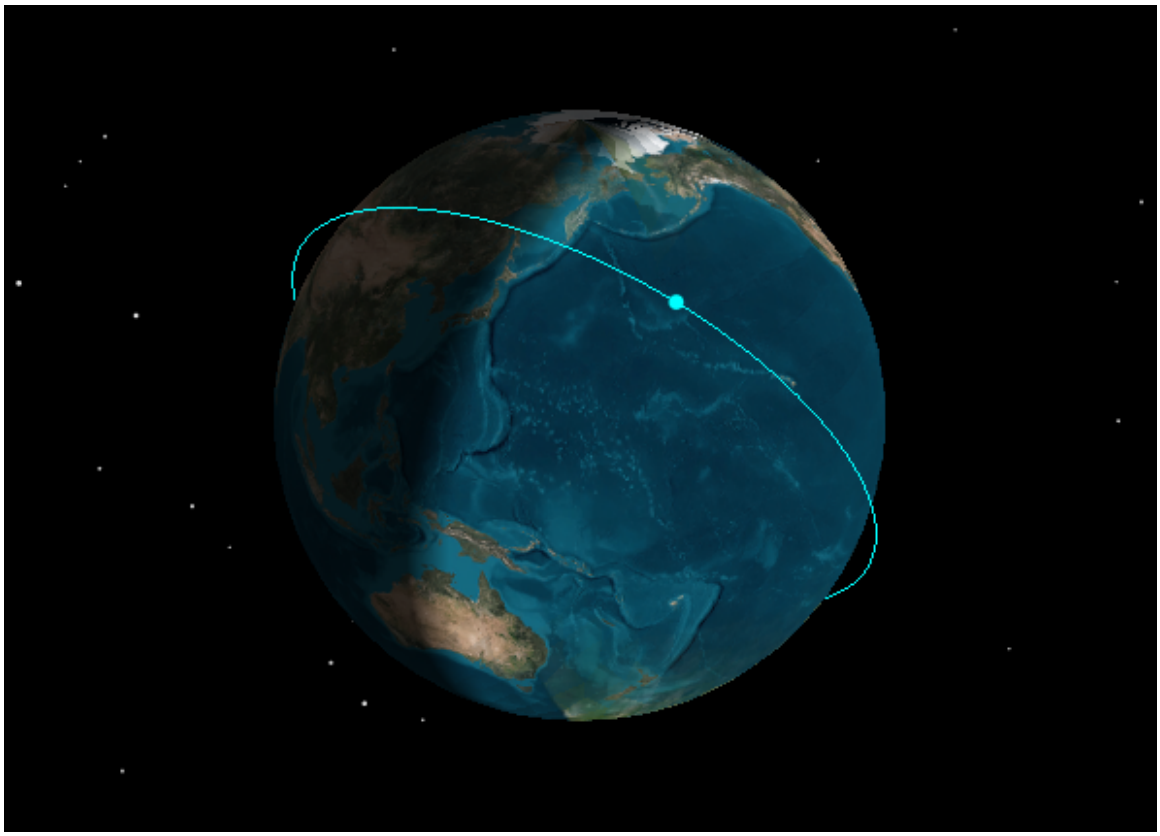

Figure 13. Orbit with Lowest Power Generation

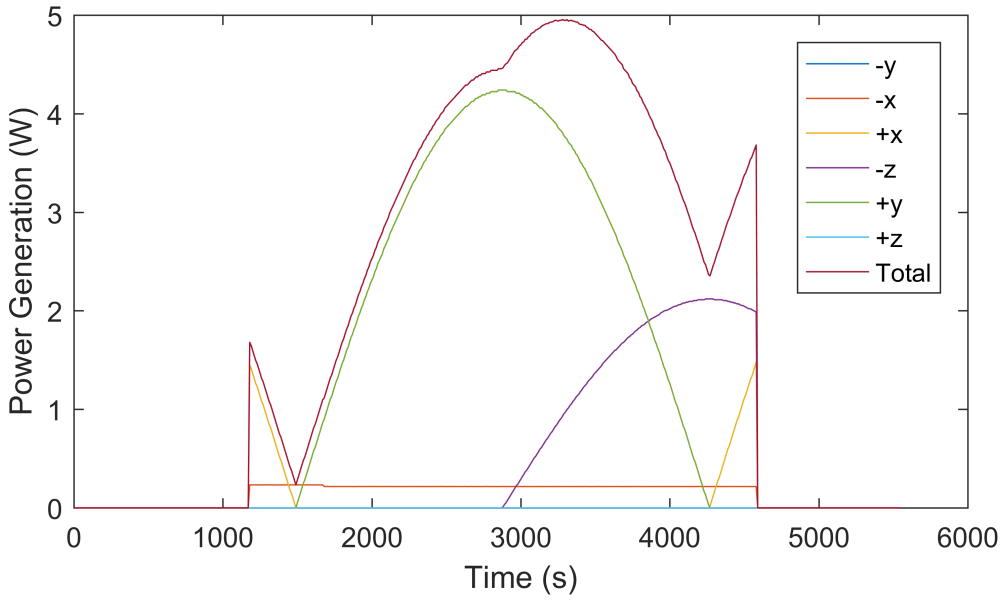

Figure 14. Power Generation by Each Panel over Time

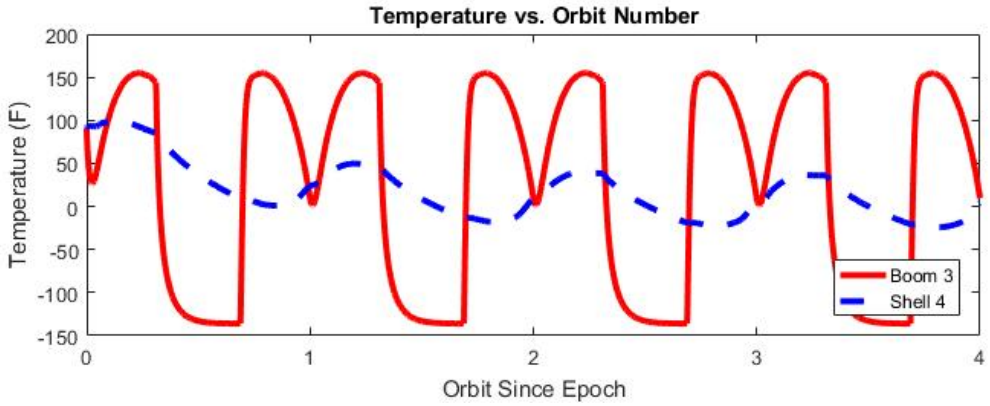

Figure 15. D3 Components Temperatures over Time

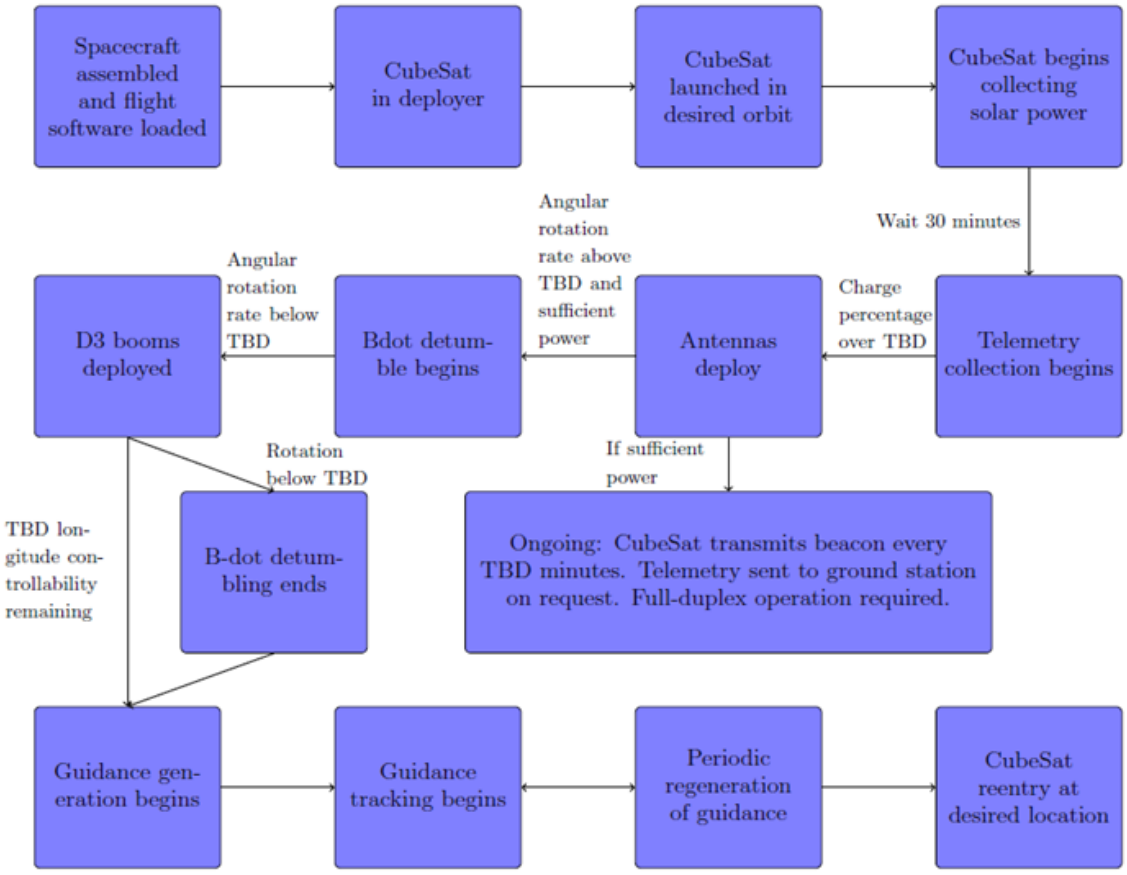

Figure 16. D3 Mission Concept of Operations

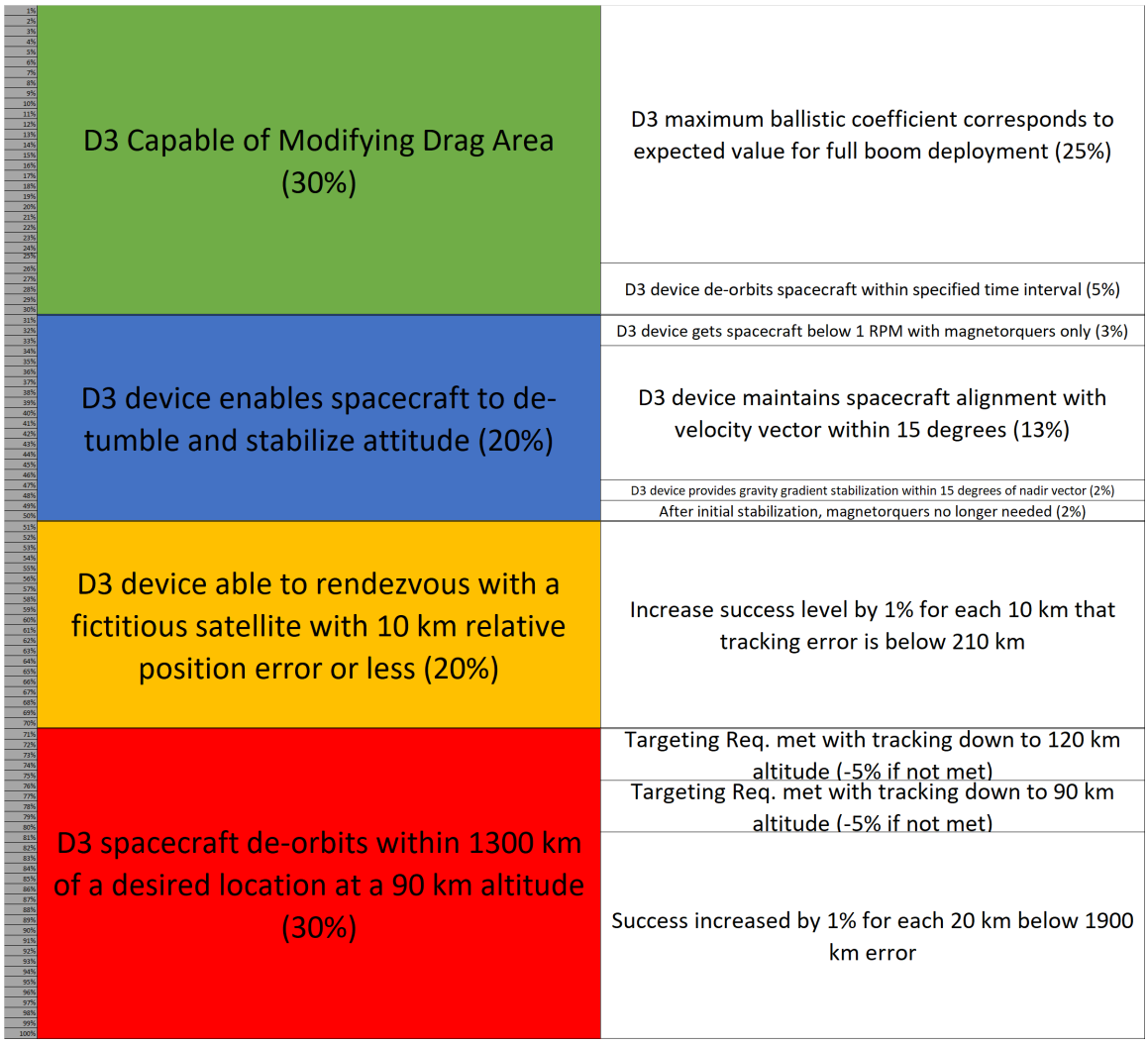

Figure 17. D3 Mission Concept of Operations

CONCLUSION

This paper presents the design of the Drag De-Orbit Device (D3) mission which will involve a 2U CubeSat with a retractable drag device that will be actively modulated to autonomously control the re-entry location of the CubeSat. The CubeSat will use commercially available TRL 9 components for the avionics, antennas, and structure with the exception of the D3 device and structural interface adapter, D3 control board, and antenna deployment mechanism. The D3 board, though made in-house, will use a high performance, multiple fault tolerant, radiation resistant, TRL9 spacecraft processor. The use of space-tested components will increase the reliability of the satellite and the chance of mission success. After launch, the spacecraft will demonstrate the operation of the drag device, orbital maneuvering using aerodynamic drag, passive attitude stabilization using aerodynamic and gravity gradient torques, and finally, controlled re-entry using aerodynamic drag. After a successful mission, the D3 device and control algorithms will hopefully become standard tools for spacecraft attitude, orbit, and de-orbit control.

ACKNOWLEDGEMENTS

The authors wish to thank a.i. solutions for sponsoring this investigation under a NASA Kennedy Space Center subcontract (project LSP 15-025: A Drag Device for Controlled De-Orbiting of LEO Spacecraft). This work was also supported by a NASA Space Technology Research Fellowship.

REFERENCES

[1] W. H. Ailor and R. P. Patera, "Spacecraft re-entry strategies: Meeting debris mitigation and ground safety requirements," *Proceedings of the Institution of Mechanical Engineers, Part G: Journal of Aerospace Engineering*, Vol. 221, June 2007, pp. 947–953, 10.1243/09544100JAERO199.

[2] NASA, "Process for Limiting Orbital Debris," Tech. Rep. NASA-STD-8719.14A, May 2012.

[3] B. Cotton, "On-Orbit Results from CanX-7 Drag Sail De-Orbit Mission," *Proceedings of the 31st Annual AIAA/USU Conference on Small Satellites*, Logan, Utah, Aug. 2017.

[4] P. Harkness, M. McRobb, P. Lützkendorf, R. Milligan, A. Feeney, and C. Clark, "Development Status of AEOLDOS – A Deorbit Module for Small Satellites," *Advances in Space Research*, Vol. 54, July 2014, pp. 82–91, 10.1016/j.asr.2014.03.022.

[5] "Re-Entry: FREEDOM Drag Sail CubeSat – Spaceflight101,"

[6] D. Guglielmo, S. Omar, R. Bevilacqua, L. Fineberg, J. Treptow, B. Poffenberger, and Y. Johnson, "DRAG DE-ORBIT DEVICE- A NEW STANDARD RE-ENTRY ACTUATOR FOR CUBESATS," Orlando, FL, Nov. 2017.

[7] M. S. Murbach, P. Papadopoulos, C. Glass, A. Dwyer-Cianciolo, R. W. Powell, S. Dutta, A. Guarneros-Luna, F. A. Tanner, and A. Dono, "Modeling the Exo-Brake and the Development of Strategies for De-Orbit Drag Modulation," 2016.

[8] S. S.-M. Swei and A. Westfall, "Attitude Control System Design for CubeSats Configured with Exo-Brake Parachute," *AIAA SPACE 2016*, American Institute of Aeronautics and Astronautics, 2016. DOI: 10.2514/6.2016-5540.

[9] S. Dutta, A. Bowes, A. M. Dwyer Cianciolo, C. Glass, and R. W. Powell, "Guidance Scheme for Modulation of Drag Devices to Enable Return from Low Earth Orbit," *AIAA Atmospheric Flight Mechanics Conference*, 2017, p. 0467, 10.2514/6.2017-0467.

[10] D. Pérez and R. Bevilacqua, "Differential Drag Spacecraft Rendezvous using an Adaptive Lyapunov Control Strategy," *Acta Astronautica*, Vol. 83, 2013, pp. 196–207, 10.1016/j.actaastro.2012.09.005.

[11] B. S. Kumar, A. Ng, K. Yoshihara, and A. D. Ruiter, "Differential Drag as a Means of Spacecraft Formation Control," *IEEE Transactions on Aerospace and Electronic Systems*, Vol. 47, Apr. 2011, pp. 1125–1135, 10.1109/TAES.2011.5751247.

[12] C. L. Leonard, W. M. Hollister, and E. V. Bergmann, "Orbital Formation Keeping with Differential Drag," *Journal of Guidance, Control, and Dynamics*, Vol. 12, Jan. 1989, pp. 108–113, 10.2514/3.20374.

[13] L. Mazal, D. Pérez, R. Bevilacqua, and F. Curti, "Spacecraft Rendezvous by Differential Drag Under Uncertainties," *Journal of Guidance, Control, and Dynamics*, Vol. 39, Aug. 2016, pp. 1721–1733, 10.2514/1.G001785.

[14] C. Foster, H. Hallam, and J. Mason, "Orbit Determination and Differential-drag Control of Planet Labs Cubesat Constellations," *Advances in the Astronautical Sciences Astrodynamics, Volume 156*, Sept. 2015. arXiv: 1509.03270.

[15] S. Omar and R. Bevilacqua, "A HYBRID ADAPTIVE CONTROL ALGORITHM FOR SPACECRAFT GUIDANCE TRACKING USING AERODYNAMIC DRAG," Orlando, FL, IAA, Nov. 2017.

[16] C. The CubeSat Program, "CubeSat Design Specification Rev. 13," Feb. 2014.

[17] J. Virgili and P. Roberts, "Atmospheric Interface Reentry Point Targeting Using Aerodynamic Drag Control," *Journal of Guidance, Control, and Dynamics*, Vol. 38, No. 3, 2015, pp. 1–11, 10.2514/1.G000884.

[18] D. A. Vallado and D. Finkleman, "A Critical Assessment of Satellite Drag and Atmospheric Density Modeling," *Acta Astronautica*, Vol. 95, Feb. 2014, pp. 141–165, 10.1016/j.actaastro.2013.10.005.

[19] P. Kovář, "piNAV L1—GPS receiver for small satellites," *Gyroscopy and Navigation*, Vol. 8, Apr. 2017, pp. 159–164, 10.1134/S2075108717020079.

[20] J.-G. Yoo, H. Jin, J.-H. Seon, Y.-H. Jeong, D. Glaser, D.-H. Lee, and R. P. Lin, "Thermal Analysis of TRIO-CINEMA Mission," *Journal of Astronomy and Space Sciences*, Vol. 29, Mar. 2012, pp. 23–31, 10.5140/JASS.2012.29.1.023.

[21] NASA, "Launch Services Program CubeSat Requirements," 2014.

[22] L. L. C. NanoRacks, "NanoRacks CubeSat Deployer (NRCSD) Interface Control Document," 2013.